Membrane repair against *H. pylori* promotes cancer cell proliferation

Li-Ling Lin[1], Hsuan-Cheng Huang[4], Satoshi Ogihara[5], Jin-Town Wang[6], Chiung-Nien Chen[3,7], Hsueh-Fen Juan[1,2]

[1]Institute of Molecular and Cellular Biology, [2]Department of Life Science, [3]Angiogenesis Research Center, National Taiwan University, Taipei 106, Taiwan. [4]Institute of Biomedical Informatics, Center for Systems and Synthetic Biology, National Yang-Ming University, Taipei 112, Taiwan. [5]Biological Science, Graduate School of Science, Osaka University, Osaka 560-0043, Japan. [6]Department of Microbiology, National Taiwan University College of Medicine, Taipei 100, Taiwan. [7]Department of Surgery, National Taiwan University Hospital, Taipei 100, Taiwan.

Membrane repair is a universal response against physical and biological insults and enables cell survival[1-3]. *Helicobacter pylori* is one of the most common human pathogens and the first formally recognized bacterial carcinogen associated with gastric cancer[4]. However, little is known about host membrane repair in the context of *H. pylori* infection. Here we show that *H. pylori* disrupts the host plasma membrane and induces Ca^{2+} influx, which triggers the translocation of annexin family members A1 and A4 to the plasma membrane. This in turn activates a membrane repair response through the recruitment of lysosomal membranes and the induction of downstream signaling transduction pathways that promote cell survival and proliferation. Based on our data, we propose a new model by which *H. pylori* infection activates annexin A1 and A4 for membrane repair and how annexin A4 over-expression induced signaling promotes cell proliferation. Continual activation of this membrane repair response signaling cascade may cause abnormal cellular states leading to carcinogenesis. This study links *H. pylori* infection to membrane repair, providing insight into potential mechanisms of carcinogenesis resulting from membrane damage.

Injury to mammalian cells by different forms of extracellular stressors evokes a survival response, whereby the cell responds via an influx of Ca^{2+}. This process

triggers many protein pathways that mediate patch vesicles and induce exocytosis of endomembranes to fuse to the site of disruption[2,5,6]. To test the hypothesis that *H. pylori* infection damages host plasma membrane integrity, we used a membrane-impermeant fluorescein isothiocyanate-dextran (FDx) as a marker for detecting membrane breaks[7]. In our study, the presence of FDx was demonstrated in the cytoplasm and at breach sites of infected cells (Fig. 1a). To exclude the possibility that the presence of intracellular dextrans were due to fluid phase endocytosis or pinocytosis induced by *H. pylori* secreting cytotoxins, we treated AGS cells with cytochalasin B, which blocks the formation of contractile microfilaments and inhibits actin polymerization[8]. We were thereby able to show that FDx was detected in non-infected cells that had not been treated with cytochalasin B (Fig. 1b), whereas FDx was undetectable with cytochalasin B treatment (Fig. 1c). Additionally, after *H. pylori* infection, FDx can be detected in the cytoplasm despite cytochalasin B treatment (Fig 1d).

Considering that Ca^{2+} plays an important role in triggering other molecules to execute wound healing[2,6], we investigated whether intracellular Ca^{2+} levels would change following *H. pylori* infection. Consistent with previous reports[9,10], our results showed increased levels of intracellular Ca^{2+} in *H. pylori* infected cells (Fig. 1e). Previous reports have demonstrated the involvement of annexin A1 in plasma

membrane repair using a blocking antibody to prevent the plasma membrane from resealing[11]. Annexins are classed as Ca^{2+} and phospholipid binding proteins by their conserved core domain, and they are implicated in membrane trafficking and vesicle aggregation[12]. To determine whether *H. pylori* infection participates in the membrane repair system, we used annexin A1 to investigate this pathway in *H. pylori* infected cells. There is currently no evidence to suggest a relationship between annexin A1 and *H. pylori* in the literature. In this investigation, we stained annexin A1 in *H. pylori* infected SC-M1 cells and measured its expression by confocal microscopy. As seen in Figure 1f, annexin A1 staining was clearly demonstrated around the plasma membrane of these cells. These results suggest that *H. pylori* infection leads to plasma membrane disruptions and is involved in the membrane repair response.

Compared to other annexins, annexin A1 and A4 have lower sensitivities to Ca^{2+}, and they require prolonged elevations of intracellular calcium concentrations ($[Ca^{2+}]i$) to associate with the intracellular membrane[13]. Previous studies have shown that binding of annexin A4 to phospholipids is dependent on Ca^{2+}. After treatment with the Ca^{2+} ionophore, ionomycin, which elevates Ca^{2+} level in the cytoplasm, annexin A4 translocates to the plasma membrane and subsequently to the nuclear membrane in three different cell lines[12,14]. To confirm the role of annexin A4

in this study, we increased intracellular Ca^{2+} levels with ionomycin in gastric cancer cells (Fig. 2a) to replicate the translocation of annexin A4 previously reported using confocal microscopy (Fig 2b). In our previous results, we had found over-expression of annexin A4 in gastric cancer patients and cells with *H. pylori* infection[15]. To determine whether annexin A4 plays an important role in the process of host cells with *H. pylori* infection, we monitored the location of annexin A4 in cells taken from two different gastric tumors, AGS and SC-M1, which were transfected with EGFP-annexin A4 (green fluorescent protein) fusion protein and then infected with Hoechst-labeled *H. pylori* by time-lapse microscopy. In the absence of infection, annexin A4 expression was abundant throughout the cell, including within the cytoplasm and nucleus (Fig. 2b). Following *H. pylori* contact with the cell surface membrane, annexin A4 gradually accumulated at the sites of infection on the plasma membrane (Fig. 2c, d and Supplementary Movie 1 and 2). We also determined the localization of annexin A1 and A4 with and without infection to explore whether similar biological processes were involved for these annexins in *H. pylori* infected host cells. Co-localization of annexin A1 and A4 was observed in the plasma membrane (Fig. 2e). These results suggest that the Ca^{2+} influx seen in *H. pylori* infection can induce annexin A1 and A4 aggregation in the plasma membrane.

To determine whether annexin A4 translocates to plasma membrane to protect

the host cell after infection, we over-expressed annexin A4 or knocked down annexin A4 expression using small interfering RNA (siRNA) in AGS cells before infection. As expected, a significant influx of FDx appeared in annexin A4-knockdown cells in comparison to control siRNA transfected cells (Fig. 3a). Additionally, greater levels of FDx were observed in the cytoplasm of cells transfected with empty vector compared to cells over-expressing annexin A4 (Fig. 3b).

Resealing of plasma membrane is facilitated by the recruitment of intercellular vesicles derived from the endoplasmic reticulum, Golgi compartment and lysosomes[16,17]. We explored the mechanisms underlying membrane fusion and looked at the differential gene expression between annexin A4 over-expressing cells and vector-expressing cells using exon array analysis. There were 47 genes (≥1.5 fold) which were classed as plasma membrane proteins in annexin A4 over-expressing cells (Supplementary Table 1). Among these genes, we used lysosomal-associated membrane protein 2 (LAMP-2), a specific marker of lysosomes[18] to determine whether *H. pylori* infection and annexin A4 are capable of recruiting lysosomal membranes to the cell surface. LAMP-2 was shown to be upregulated by annexin A4 using immunoblotting assay (Fig 3c). Following flow cytometry analysis, we found that the cell surface of infected cells expressed more

LAMP-2 compared to non-infected cells (Fig. 3d). When we evaluated the influence of annexin A4 on LAMP-2 translocation to the cell surface, we found that annexin A4 over-expression increased LAMP-2 expression on the surface of infected cells (Fig. 3e). This is in contrast to the silencing annexin A4 (Fig. 3f). Based on this data, it is possible that annexin A4 inhibits membrane lesions by recruiting lysosome membranes to promote the plasma membrane repair response (Supplementary Movie 3). Over-expression of annexin A4 has been reported as a feature in different types of cancer, including gastric cancer[15,19]. However, the mechanism of annexin A4 associated with gastric cancer is not clear.

To elucidate the role of annexin A4 in carcinogenesis, we also performed exon array for downstream genes expressed in annexin A4-over-expressing cells. Exon array offers a more accurate view of gene-level expression with four probes per exon[20]. Among the annexin A4-induced plasma membrane proteins (Supplementary Table 1), hyaluronan-mediated motility receptor (RHAMM), an oncogene that has been shown to be over-expressed in several cancers, including gastric cancer[21], showed increased gene expression (fold change = 2.4). Moreover, its differential expression was supported by immunoblotting (Fig. 4a). RHAMM has been implicated in many cellular processes including signaling, cell proliferation, and tumorigenesis[22]. In signaling transduction, RHAMM has been reported to induce the

RAS signaling cascade[23] and is downregulated by tumor suppressor p53[24]. The RAS signaling cascade transduces downstream signals by activating phospho-Akt through PI3K. Here, we found that annexin A4 activated phospho-Akt (Fig. 4b) and downregulated p53 and p21 expression using immunoblotting assay (Fig. 4c). Previous studies have shown that p53 expression is degraded by MDM2 which is induced by phospho-Akt activation[25]. We found that annexin A4 upregulates MDM2 as consistent with previous findings (Fig. 4d).

Using the IPA database, we performed gene function analysis of the microarray data and found that 25 of 42 genes (≥ 2 fold differential expression, *t*-test, $p<0.05$) (Supplementary Table 2) were eligible for network function analysis. The top ranked network was "cancer, cell cycle, and reproductive system disease" (Supplementary Fig. 1a), and the top-ranked disease was "cancer" (Supplementary Fig. 1b). Cyclin-dependent kinase 1 (CDC2) and PDZ binding kinase (PBK) were classed as cancer-related genes in annexin A4 over-expressing cells (Supplementary Fig. 1b and Table 2) and involved in the annexin A4 inducing model. These differences were supported using qRT-PCR analysis (Fig. 4d). The mutual activation of CDC2 and PBK has been reported[26] and p53 mediates the G2/M phase checkpoint via activation of p21 to inhibit CDC2[27]. CDC2 activation inhibits G2/M phase arrest to maintain mitosis and enables cell proliferation. In cell proliferation

assays, annexin A4 overexpressing cells increased the growth rate significantly (p<0.001) (Fig. 4e) whereas annexin A4 knockdown decreased the growth rate significantly (p<0.001) (Fig. 4f). This may explain why long-term *H.pylori* infection increases cell growth and induces gastric cancer in mongolian gerbils[28]. Taken together, our results indicate that annexin A4 over-expression induces RHAMM to activate phospho-Akt, which then upregulates MDM2 to suppress p53 and p21. This subsequently raises PBK and CDC2 expression and ultimately causes cell proliferation and carcinogenesis (Fig. 4g).

In this study, we showed that annexin A4 is involved in the membrane repair response during *H. pylori* infection and when over-expressed, has the proliferation capacity to induce downstream signals to respond to long-term infection. Our study provides insight into the membrane repair response induced in host cell during bacterial infection. However, over-expression of these proteins and the maintenance of their activation in the host cell may predispose to carcinogenesis. The findings of this study provide a potential new target for gastric cancer therapy directed at blocking these membrane repair associated proteins.

METHODS SUMMARY

Plasmids and transfections. pcDNA3.1(+)/pEGFP-C1-annexin A4 and annexin A4 specific siRNA (Stealth™ RNAi, Invitrogen) in AGS (CRL-1739) or SC-M1 cells

were utilized in this study. Cells were grown as described in Methods, and transiently transfected following the manufacturer's instructions. After transfection for 48 hours, differential expression of proteins and genes were detected.

Bacteria. *H. pylori* (NTUH-GC05) strain ($cagA^+/vacA^+$) was isolated from the stomach of a gastric cancer male patient. The multiplicity of infection for all infection experiments was 150.

Immunofluorescence. To determine annexin A4 localization in host cells after *H. pylori* infection, cells were transfected with pEGFP-C1-annexin A4 before infection. *H. pylori* were stained with Hoechst 33258. Fluorescence images of living cells were captured by real-time fluorescence microscopy. Cells were treated with cytochalasin B before infection, or treated with FDx after infection to observe disruption sites. After infection, cells were fixed and incubated with appropriate primary and secondary antibodies. Immunostaining of cells were imaged by confocal microscopy (Zeiss LSM 510).

Cell proliferation assay. AGS cells were loaded in a 96-well microtiter E-plate and transfected with expression vectors or siRNAs. Cells were then monitored for a total of 84 hours. The level of cell proliferation is shown as cell index (CI) based on measured electrical impedance by xCELLigence system (Roche). All detailed experimental procedures are described in Methods.

1 Divangahi, M. *et al.* Mycobacterium tuberculosis evades macrophage defenses by inhibiting plasma membrane repair. *Nature immunology* **10**, 899-906 (2009).

2 McNeil, P. L. & Kirchhausen, T. An emergency response team for membrane repair. *Nat Rev Mol Cell Biol* **6**, 499-505 (2005).

3 Roy, D. *et al.* A process for controlling intracellular bacterial infections induced by membrane injury. *Science (New York, N.Y* **304**, 1515-1518 (2004).

4 Blaser, M. J. Linking Helicobacter pylori to gastric cancer. *Nature medicine* **6**, 376-377 (2000).

5 McNeil, P. Membrane repair redux: redox of MG53. *Nature cell biology* **11**, 7-9 (2009).

6 Bi, G. Q., Alderton, J. M. & Steinhardt, R. A. Calcium-regulated exocytosis is required for cell membrane resealing. *The Journal of cell biology* **131**, 1747-1758 (1995).

7 McNeil, P. L. & Ito, S. Gastrointestinal cell plasma membrane wounding and resealing in vivo. *Gastroenterology* **96**, 1238-1248 (1989).

8 Theodoropoulos, P. A. *et al.* Cytochalasin B may shorten actin filaments by a mechanism independent of barbed end capping. *Biochemical pharmacology* **47**, 1875-1881 (1994).

9 Beil, W., Obst, B., Wagner, S. & Sewing, K. F. The Helicobacter pylori fatty acid cis-9,10-methyleneoctadecanoic acid stimulates protein kinase C and increases DNA synthesis of gastric HM02 cells. *British journal of cancer* **77**, 1852-1856 (1998).

10 Marlink, K. L. *et al.* Effects of Helicobacter pylori on intracellular Ca2+ signaling in normal human gastric mucous epithelial cells. *American journal of physiology* **285**, G163-176 (2003).

11 McNeil, A. K., Rescher, U., Gerke, V. & McNeil, P. L. Requirement for annexin A1 in plasma membrane repair. *The Journal of biological chemistry* **281**, 35202-35207 (2006).

12 Gerke, V., Creutz, C. E. & Moss, S. E. Annexins: Linking Ca2+ signalling to membrane dynamics. *Nat Rev Mol Cell Biol* **6**, 449-461 (2005).

13 Monastyrskaya, K., Babiychuk, E. B. & Draeger, A. The annexins: spatial and temporal coordination of signaling events during cellular stress. *Cell Mol Life Sci* **66**, 2623-2642 (2009).

14 Piljic, A. & Schultz, C. Annexin A4 self-association modulates general

membrane protein mobility in living cells. *Molecular biology of the cell* **17**, 3318-3328 (2006).

15 Lin, L. L. *et al.* Annexin A4: A novel molecular marker for gastric cancer with Helicobacter pylori infection using proteomics approach. *Proteomics Clinical Applications* **2**, 619-634 (2008).

16 Togo, T., Alderton, J. M., Bi, G. Q. & Steinhardt, R. A. The mechanism of facilitated cell membrane resealing. *Journal of cell science* **112 (Pt 5)**, 719-731 (1999).

17 Rodriguez, A., Webster, P., Ortego, J. & Andrews, N. W. Lysosomes behave as Ca2+-regulated exocytic vesicles in fibroblasts and epithelial cells. *The Journal of cell biology* **137**, 93-104 (1997).

18 Fukuda, M. Lysosomal membrane glycoproteins. Structure, biosynthesis, and intracellular trafficking. *The Journal of biological chemistry* **266**, 21327-21330 (1991).

19 Mussunoor, S. & Murray, G. I. The role of annexins in tumour development and progression. *The Journal of pathology* **216**, 131-140 (2008).

20 Kapur, K., Xing, Y., Ouyang, Z. & Wong, W. H. Exon arrays provide accurate assessments of gene expression. *Genome biology* **8**, R82 (2007).

21 Li, H. *et al.* Expression of hyaluronan receptors CD44 and RHAMM in stomach cancers: relevance with tumor progression. *International journal of oncology* **17**, 927-932 (2000).

22 Maxwell, C. A., McCarthy, J. & Turley, E. Cell-surface and mitotic-spindle RHAMM: moonlighting or dual oncogenic functions? *Journal of cell science* **121**, 925-932 (2008).

23 Hall, C. L. *et al.* Overexpression of the hyaluronan receptor RHAMM is transforming and is also required for H-ras transformation. *Cell* **82**, 19-26 (1995).

24 Sohr, S. & Engeland, K. RHAMM is differentially expressed in the cell cycle and downregulated by the tumor suppressor p53. *Cell cycle (Georgetown, Tex* **7**, 3448-3460 (2008).

25 Ogawara, Y. *et al.* Akt enhances Mdm2-mediated ubiquitination and degradation of p53. *The Journal of biological chemistry* **277**, 21843-21850 (2002).

26 Gaudet, S., Branton, D. & Lue, R. A. Characterization of PDZ-binding kinase, a mitotic kinase. *Proceedings of the National Academy of Sciences of the United States of America* **97**, 5167-5172 (2000).

27 Agarwal, M. L., Agarwal, A., Taylor, W. R. & Stark, G. R. p53 controls both the G2/M and the G1 cell cycle checkpoints and mediates reversible growth

arrest in human fibroblasts. *Proceedings of the National Academy of Sciences of the United States of America* **92**, 8493-8497 (1995).

28 Watanabe, T., Tada, M., Nagai, H., Sasaki, S. & Nakao, M. Helicobacter pylori infection induces gastric cancer in mongolian gerbils. *Gastroenterology* **115**, 642-648 (1998).

Supplementary Information is linked to the online version of the paper at www.nature.com/nature.

Acknowledgements We would like to thank Cho-Yi Chen for assistance with statistics analyses, Meng-Ting Tsai for help with drawing supplementary Movie 3 and the staff of the Second Core Lab, Department of Medical Research, National Taiwan University Hospital for technical support. This work was supported by National Science Council of Taiwan (NSC 97-2311-B-002-010-MY3), Frontier and Innovative Research of National Taiwan University (98R0313) and the National Health Research Institutes, Taiwan (NHRI-EX98-9819PI).

Author Contributions L.L.L. and H.F.J. designed the research. L.L.L carried out the experiments. H.C.H. assisted construction of the signaling transduction. L.L.L., H.C.H., C.N.C. and H.F.J. discussed the results and wrote the manuscript. S.O. discussed the results in membrane repair. J.T.W. assisted with *H. pylori* infection experiments. C.N.C. and H.F.J. provided funding for the study.

Author Information Correspondence and requests for materials should be addressed to C.N.C. (cnchen@ntu.edu.tw) or H.F.J. (yukijuan@ntu.edu.tw).

Figure Legends

Figure 1 | **Plasma membrane microinjury, intracellular Ca^{2+} level elevation and annexin A1 translocation in cells are caused by *H. pylori* infection. a**-**d**, Plasma membrane integrity in cells labeled with fluorescein isothiocyanate-dextran (FDx; green) were monitored. **a**, FDx was detected in AGS and SC-M1 cells after *H. pylori* (labeled with Cy 5; blue) infection. **b-d**, AGS cells were treated with cytochalasin B. **b**, Without cytochalasin B treatment, fewer FDx were seen along the plasma membrane of non-infected cells. The nucleus was stained with Hoechst 33258 (blue) **c**, With cytochalasin B treatment, FDx were not observed in non-infected cells, (**d**) but were found in the infection sites and cytoplasm of host cells after *H. pylori* (labeled with TRITC; red) infection. **e**, AGS cells were loaded with Fluo-3/AM to monitor intracellular Ca^{2+} level by flow cytometry. **f**, Immunofluorescence showed that annexin A1 (labeled with FITC; green) translocated to the plasma membrane of SC-M1 cells after *H. pylori* (labeled with Cy5; blue) infection. Scale bar, 10 μm.

Figure 2 | **Dynamic localization of annexin A4 in the living cell and co-localization of annexin A1 and A4 in the plasma membrane after *H. pylori* infection. a**, Cells were treated with ionomycin (calcium ionophore, 5

μM). Ca^{2+} increases in the cells was measured using flow cytometry. **b**, Immunofluorescence showed that the localization of annexin A1 (labeled with FITC; green) and A4 (labeled with TRITC; red) was changed in the ionomycin-treated cells using confocal microscopy. Scale bar, 2 μm. **c**-**d**, Real-time fluorescence images showed localization of EGFP-annexin A4 in the living cell, (**c**) AGS and (**d**) SC-M1, after *H. pylori* infection ((yellow arrow) stained with Hoechst 33258). Films were collected from Supplementary Movie 1 (**c**, AGS cells) and Supplementary Movie 2 (**d**, SC-M1 cells), which indicate that annexin A4 aggregates to the sites of infection and the plasma membrane. **e**, Immunofluorescence of annexin A1 (labeled with FITC; green) co-localized with annexin A4 (labeled with TRITC; red) in the plasma membrane of AGS and SC-M1 cells after *H. pylori* (labeled with Cy5; blue) infection. The translocation of annexin A1 and A4 after *H. pylori* infection is marked by a white arrow.

Figure 3 | Annexin A4 participates in plasma membrane repair by recruiting lysosome-derived vesicles

a-b, Fluorescence images of FDx levels in AGS cells with *H. pylori* (labeled with Cy5 dye; red) infection showed the impact of annexin A4 on membrane microinjury. **a**, Knockdown of annexin A4 increased FDx into the cytoplasm.

On the contrary, (**b**) over-expression of annexin A4 decreased FDx in the cell. Scale bar, 10 μm. **c**, Immunoblotting of LAMP-2 expression were shown in annexin A4 over-expressing cells and in annexin A4 knockdown cells. **d**, LAMP-2 fluorescence on the surface of cells were enhanced in AGS cells after *H. pylori* infection compared with non-infected cells. **e**-**f**, Representative flow cytometry analysis of LAMP-2 in cells (**e**) over-expressing annexin A4 compared to (**f**) silencing annexin A4, and the analysis indicated that annexin A4 promotes LAMP-2 expression on the surface of infected cells.

Figure 4 | **Annexin A4 induces downstream signaling transduction which leads to cell proliferation. a**-**c,** Representative immunoblots showing the expression of (**a**) RHAMM, (**b**) phospho-AKT (Ser473) and (**c**) p53 and p21 are regulated by annexin A4 in AGS cells. **d**, qRT-PCR assay in AGS cells after enforced annexin A4 expression (black boxes) was performed to confirm exon array data (grey boxes). These relative mRNA levels of CDC2, PBK, MDM2 and TP53 were measured and normalized to GAPDH. **e-f**, For the cell proliferation assay, AGS cells ($1x10^4$ cells/well) were plated at a 96-well microtiter E-Plate. After incubation for 24 hours, the cell growth rate of (**e**) cells over-expressing annexin A4 and (**f**) cells with siRNA known down of annexin A4 were measured using xCELLigence real-time cell analyzer

system. Annexin A4 regulated cell index in a time-dependent manner. Data were normalized at the time of 24 hours, the starting transfection time, and *p*-values were calculated using the two sample Kolmogorov-Smirnov test. The mean and standard deviation of each detection time is from three independent experiments. **g**, The model responds to the annexin A4 function in the cell infected with *H. pylori*. Thus, when annexin A4 is over-expressed in the cell, this could lead to cellular proliferation by downstream signaling transduction. The expression of RHAMM, AKT, MDM2, PBK and CDC2 were upregulated (shown in a red oval plate) and p53 and p21 were down-regulated (shown in a green oval plate) by annexin A4. Ras and PI3K were supported in previous reports (shown in a blue oval plate).

METHODS

Cell lines and culture conditions. Human stomach adenocarcinoma AGS (CRL-1739; ATCC) and SC-M1 (cultured from a poorly differentiated adenocarcinoma that showed no metastasis to lymph nodes or adjacent organs)[29] cells, were grown in 90% RPMI 1640 medium (biological industries) supplemented with 1% penicillin/streptomycin and 10% fetal bovine serum (biological industries). Cells were cultured at 37 ^{o}C in an incubator with controlled humidified atmosphere containing 5% CO2.

Bacteria. *H. pylori* (NTUH-GC05) strain ($cagA^{+}$/$vacA^{+}$) was isolated from the stomach of a gastric cancer male patient at National Taiwan University Hospital and generously provided by Dr. Yo-Ping Lai. The character of the strain has previously been described[30,31]. *H. pylori* was grown on Columbia blood agar (BD) containing 5% sheep blood and incubated for 2–3 days in microaerophilic conditions (5% O_2, 10% CO_2, 85% N_2) at 37 ^{o}C.

Plasmids and transfections. The full length of annexin A4 was amplified by PCR with the following primers, forward: 5'-ATATAAGCTTGCCACCATGGCCATGGCAACCAAA-3' and reverse: 5'-GCGCGGGAATTCTTAATCATCTCCTCCACA-3', and inserted into the HindIII/EcoRI sites of pcDNA3.1(+) (Invitrogen). For immunofluorescence analysis, annexin A4 was amplified by PCR with the following primers: forward:

5’-ATATAAGCTTGCCACCATGGCCATGGCAACCAAA-3’ and reverse: 5’-AGCGCGCCTGCAGTTAATCATCTCCTCCACA-3’, and inserted into the HindIII/pst I sites of pEGFP-C1 (BD Clontech). Annexin A4 specific siRNA and negative control Stealth siRNA were purchased from Invitrogen (Stealth™ RNAi). Cells were plated in 6-well plates or coated cover slips for 24 hours. Cells were then transiently transfected with pcDNA 3.1(+)/pEGFP-C1-annexin A4 (8 μg for 6-well plate (each well); 0.4 μg for 96-well E-plate (each well)) or annexin A4 siRNA (100 pmole for 6-well plate (each well); 10 pmole for 96-well E-plate (each well)) using Lipofectamine 2000 (Invitrogen) following the manufacturer's instructions. Expression vector and siRNA transfection efficiency was determined by qRT-PCR and immunoblotting. After transfection for 48 hours, differential expression of proteins and genes were detected.

Antibodies. The mouse monoclonal antibodies used in this study include: annexin A1 (sc-12740) and p53 (sc-126) form Santa Cruz Biotechnology, LAMP-2 (ab25631) and RHAMM (ab67003) from Abcam, IgG-1 isotype (555746; BD), α-tubulin (T5168; Sigma). The rabbit polyclonal antibodies included: *H. pylori* (AHP602H; AbD serotec), annexin A4 (sc-28827) and p21 (sc-397) from Santa Cruz Biotechnology, Akt (9272) and phospho-Akt (Ser473; 9271S) from Cell Signaling Technology. The goat polyclonal antibody included: annexin A4 (sc-1930; Santa

Cruz Biotechnology).

Living cell imaging. To determine annexin A4 localization after *H. pylori* infection, AGS or SC-M1 cells (3×10^5/well) were plated in coated chamber slides (Nunc). After 24 hours incubation, cells were transfected with pEGFP-C1-annexin A4 (8 μg) for 48 hours before infection. *H. pylori* were re-suspended with serum-free culture medium and stained with Hoechst 33258 (Sigma) for 1 hour, centrifuged, washed twice and then re-suspended with fresh serum-free culture medium. Cultured cells were replaced with fresh serum-free culture medium (1 ml per well) and infected with *H. pylori* at a multiplicity of infection (MOI) of 150. Fluorescence images of living cells were captured by fluorescence microscopy (SC-M1: Zeiss Axiovert 200M with 100x oil lens; AGS: Nikon A1 confocal microscopy with 60x oil lens). Images were arranged by using MetaMorph (Molecular Devices) software.

Confocal microscopy. Cells (8×10^5 cells/well) were plated onto glass cover slips coated with poly-L-lysine in 6-well plates. To observe disruption site, cells were treated with cytochalasin B (10 μg/ml) for 1 hour before infection, or treated with FDx (5 mg/ml; 10 kDa) for 30 min after infection for 2.5 hours. After infection (MOI = 150) for 3 hours, cells were fixed with 4% paraformaldehyde for 15 minutes, permeabilized with 1% Triton-X-100 in PBS for 30 minutes and blocked with 0.1% BSA/PBS overnight at 4 ^{o}C. Cells were incubated with mouse anti-annexin A1

antibody (1:100), goat anti-annexin A4 antibody (1:100) or rabbit anti-*H. pylori* antibody (100 μl) for 1 hour at room temperature. After washing, secondary antibodies: FITC-labeled anti-mouse antibody (Sigma), TRITC-labeled anti-goat antibody (Sigma) or Cy5-labeled anti-rabbit antibody (Millipore) were used at 1:100 dilution and applied for 1 hour at room temperature. The cover slips were then washed and mounted onto slides. Immunostaining of cells were observed by confocal microscopy with a Plan-Apochromat 63x/1.40 oil M27 objective (Zeiss LSM 510)

Exon array hybridization and analysis. We compared the gene expression profiles between the cells transfected with pcDNA3.1(+)/annexin A4 and control (empty vector) to study the annexin A4 involved downstream genes using Exon array technique. Total cellular RNA was extracted with the use of TRIzol reagent (Invitrogen) and purity was confirmed by spectrophotometry (A_{260}/A_{280} ratio) and capillary electrophoresis (Agilent 2100 Bioanalyzer, Agilent). RNA processing and hybridization onto Affymetrix Human Exon 1.0 ST arrays were performed according to the manufacturer's protocol. Microarray (n = 2 per group) analysis was performed using Partek Genomics Suite version 6.5 (Partek Inc.). CEL data were normalized using RMA and statistically tested using *t*-tests and a total of 1052 gene expressions were found to be significantly different ($p<0.05$). To identify the function and

biological mechanism of data, we applied Ingenuity Pathway Analysis (IPA) database version 7.5, a score of 3 or above is considered statistically significant ($p<0.01$), to annotate the information.

Flow Cytometry. Measurement of intercellular [Ca^{2+}]i in infected cells (MOI = 150) for 3 hours and non infected cells were washed in HBSS buffer and then loaded with 4 μM of the Ca^{2+} indicator, Fluo-3-AM /pluronic acid F-127, for 1 hour at 37 ^{o}C. Subsequently, cells were harvested by trypsin and then resuspended in HBSS buffer. The Ca^{2+} ionophore, ionomycin (5 μM) was added to cells and cultured for 10 minutes as a positive control of increased Ca^{2+} in the cytoplasm. To determine the expression of cell surface LAMP-2, cells were re-suspended in PBS and then fixed with 2% paraformaldehyde, centrifuged, washed in PBS and blocked with 2% BSA/PBS for 15 minutes. The mouse anti-LAMP-2 antibody and mouse IgG-1 isotype control (Supplementary Fig. 2) was used at 1:200 dilution for 30 minutes at room temperature, washed and then stained with anti-FITC secondary antibody for 30 minutes at RT. Cells were washed and fixed with 4% paraformaldehyde. Fluorescence intensity was determined by FACscalibur System (BD Biosciences) and the data of each sample was analyzed using at least 10,000 cells.

Immunoblotting. Cell lysates were prepared from AGS cells (8×10^5 cells/well in 6-well plates) which were transiently transfected with the expression vectors pcDNA

3.1(+)-annexin A4 (8 μg) or annexin A4 siRNA (100 pmole). Samples were separated by 10% SDS-PAGE and then transferred onto PVDF membranes (Millipore). After blocking in 5% nonfat milk and TBST containing 0.1% Tween 20 (JT Baker) for 1 hour at room temperature with gentle rocking, the primary antibodies used were: anti-annexin A4 (1:1,000), p53 (1:1,000), p21 (1:500) antibody, Akt (1:500), phospho-Akt (Ser473; 1:500) antibody, and RHAMM antibody (1:400). Membranes were incubated with secondary antibodies of goat anti-mouse conjugated IgG (Sigma) or goat anti-rabbit conjugated IgG (Rockland), respectively. α-tubulin (1:4,000) was used as internal control. Immunoblots were visualized with the ECL detection kit (Millipore) and exposed to X-ray film. The intensity of observed bands was normalized to α-tubulin intensity. The analysis was performed using Kodak 1-D Image Analysis software version 3.6 (Eastman Kodak).

Quantitative real-time PCR. qRT-PCR was used to confirm the exon array data which were analyzed by Partek software and Ingenuity Pathway Analysis database. RNA was isolated with TRIzol (Invitrogen) from AGS cells using the RNeasy Mini Kit (Qiagen) following the manufacturer's instructions. First-strand cDNA was synthesized with total mRNA by reverse transcription kit (Invitrogen). Primers (Supplementary Table 3) were designed using the DNAStar software (DNAStar) and PrimerBank (http://pga.mgh.harvard.edu/primerbank). Gene expression was

measured with a Bio-Rad iQ5 real-time PCR detection system with an SYBR Green Supermix (Bio-Rad Laboratories) and normalized to GAPDH.

Cell proliferation assay. AGS cells (1×10^4 cells/well) were loaded at each well of a 96-well microtiter E-plate. Microelectronic sensor arrays are at the bottom of each well to detect the cell index. After incubation for 24 hours, cells were transfected with expression vectors or siRNAs for 6 hours and kept to monitor for total 84 hours. The E-plate was plated in the Real-Time Cell Analyzer (RTCA) System and incubated in an incubator containing 37 ^{o}C, 5% CO_2. The level of cell proliferation is shown as cell index (CI) based on measured electrical impedance by xCELLigence system (Roche).

29 Tzeng, C. C., Meng, C. L., Jin, L. & Hsieh, H. F. Cytogenetic studies of gastric adenocarcinoma. *Cancer genetics and cytogenetics* **55**, 67-71 (1991).

30 Lai, Y. P., Yang, J. C., Lin, T. Z., Wang, J. T. & Lin, J. T. CagA tyrosine phosphorylation in gastric epithelial cells caused by Helicobacter pylori in patients with gastric adenocarcinoma. *Helicobacter* **8**, 235-243 (2003).

31 Lai, Y. P., Yang, J. C., Lin, T. Z., Lin, J. T. & Wang, J. T. Helicobacter pylori infection and CagA protein translocation in human primary gastric epithelial cell culture. *Helicobacter* **11**, 451-459 (2006).

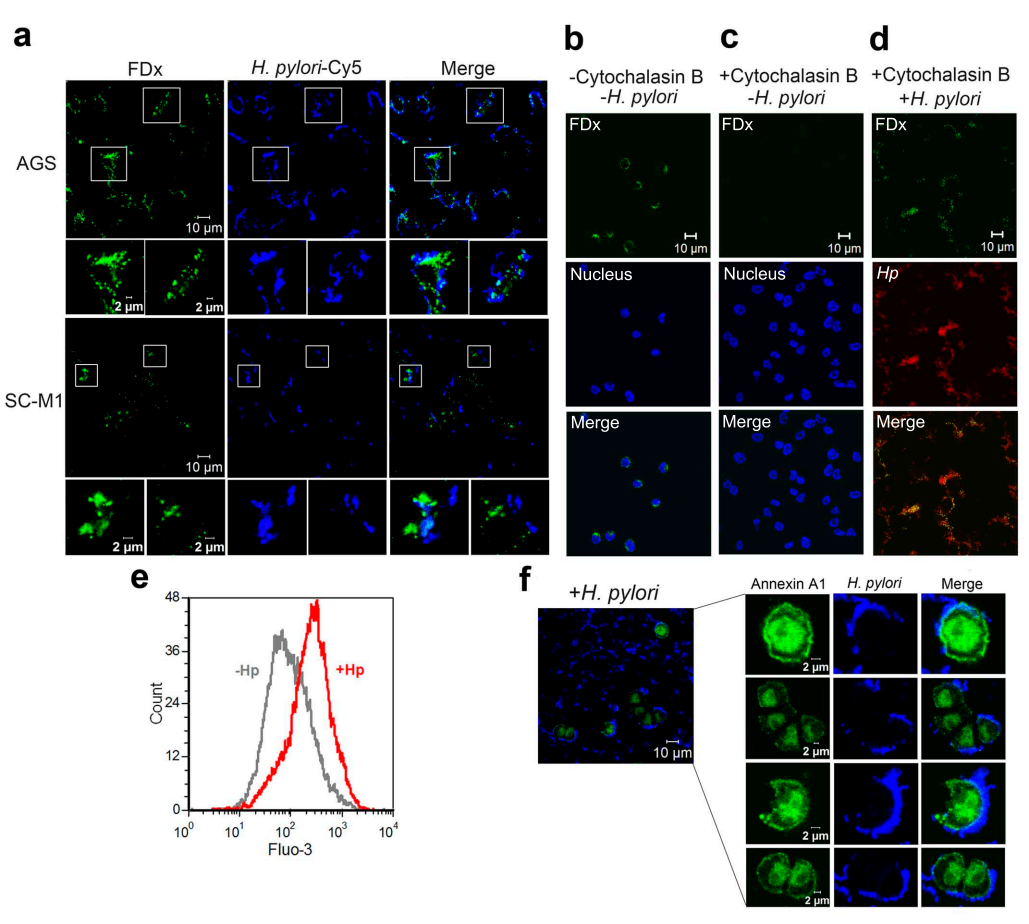
a
FDx
H. pylori-Cy5
Merge
AGS
SC-M1
10 μm
2 μm
b
-Cytochalasin B
-H. pylori
c
+Cytochalasin B
-H. pylori
d
+Cytochalasin B
+H. pylori
FDx
Nucleus
Hp
Merge
e
Count
-Hp
+Hp
Fluo-3
f
+H. pylori
Annexin A1
H. pylori
Merge

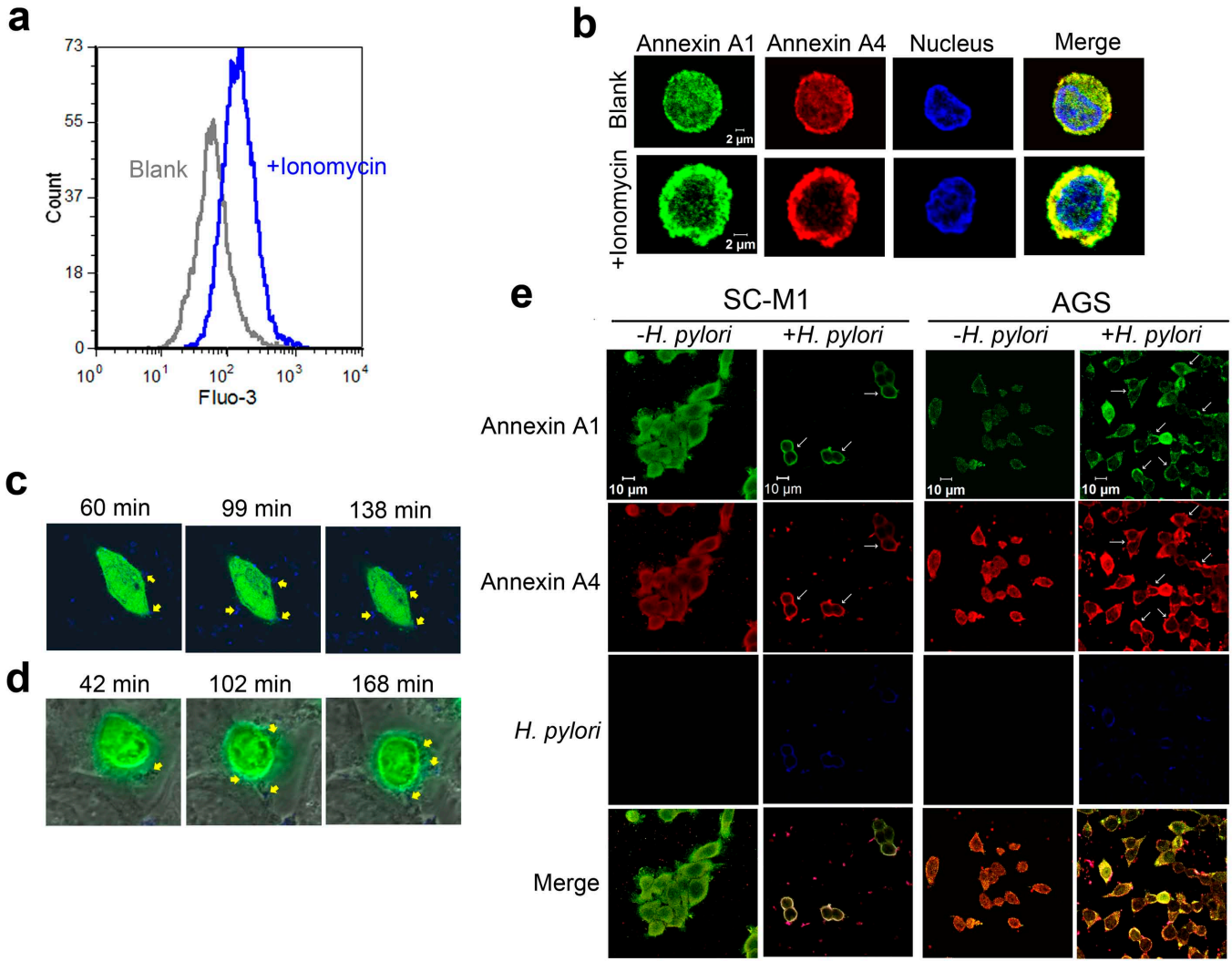
a
Count
Fluo-3
Blank
+Ionomycin
b
Annexin A1
Annexin A4
Nucleus
Merge
Blank
+Ionomycin
2 μm
c
60 min
99 min
138 min
d
42 min
102 min
168 min
e
SC-M1
AGS
-H. pylori
+H. pylori
Annexin A1
Annexin A4
H. pylori
Merge
10 μm

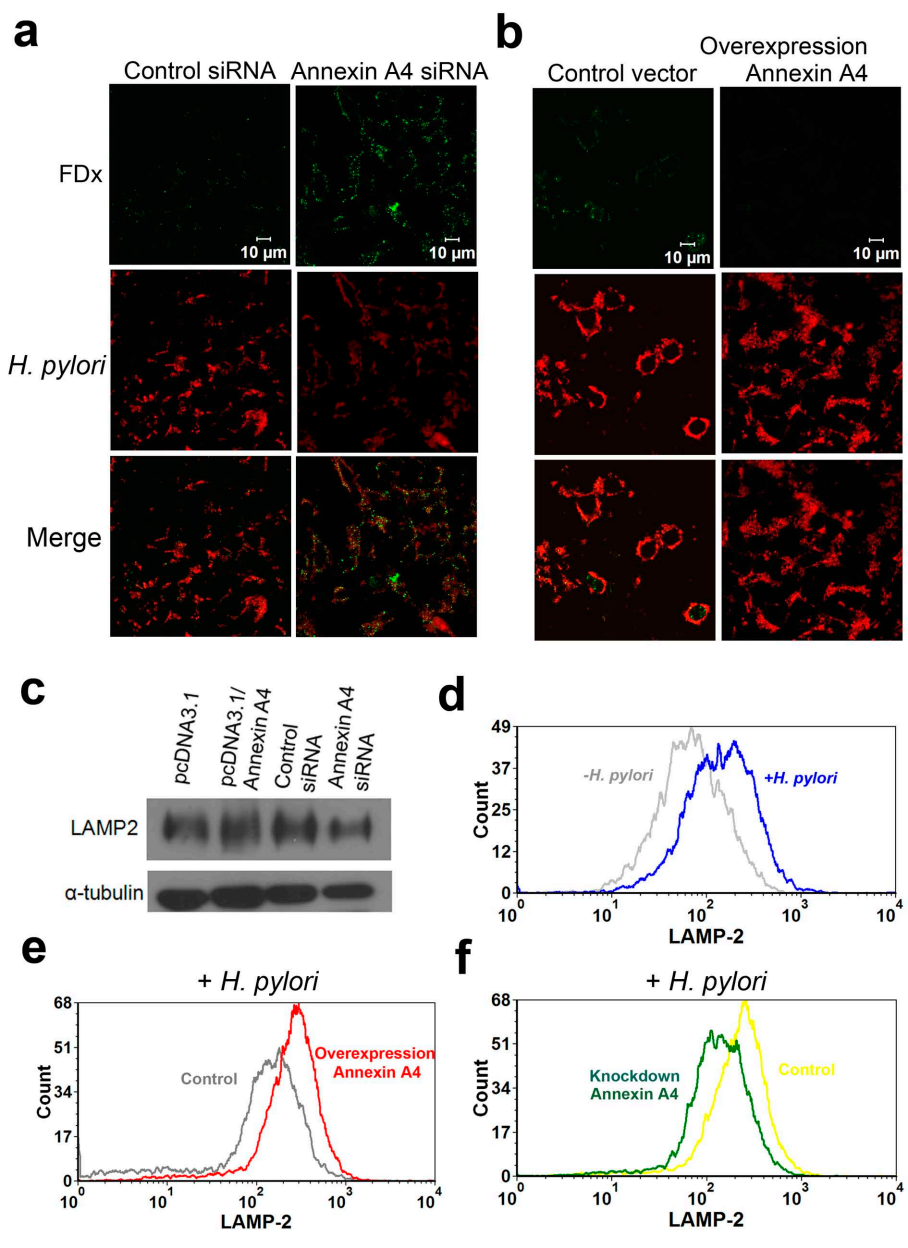
a
Control siRNA
Annexin A4 siRNA
FDx
H. pylori
Merge
10 μm
b
Overexpression
Control vector
Annexin A4
c
pcDNA3.1
pcDNA3.1/ Annexin A4
Control siRNA
Annexin A4 siRNA
LAMP2
α-tubulin
d
-H. pylori
+H. pylori
Count
LAMP-2
e
+ H. pylori
Control
Overexpression Annexin A4
f
+ H. pylori
Knockdown Annexin A4
Control

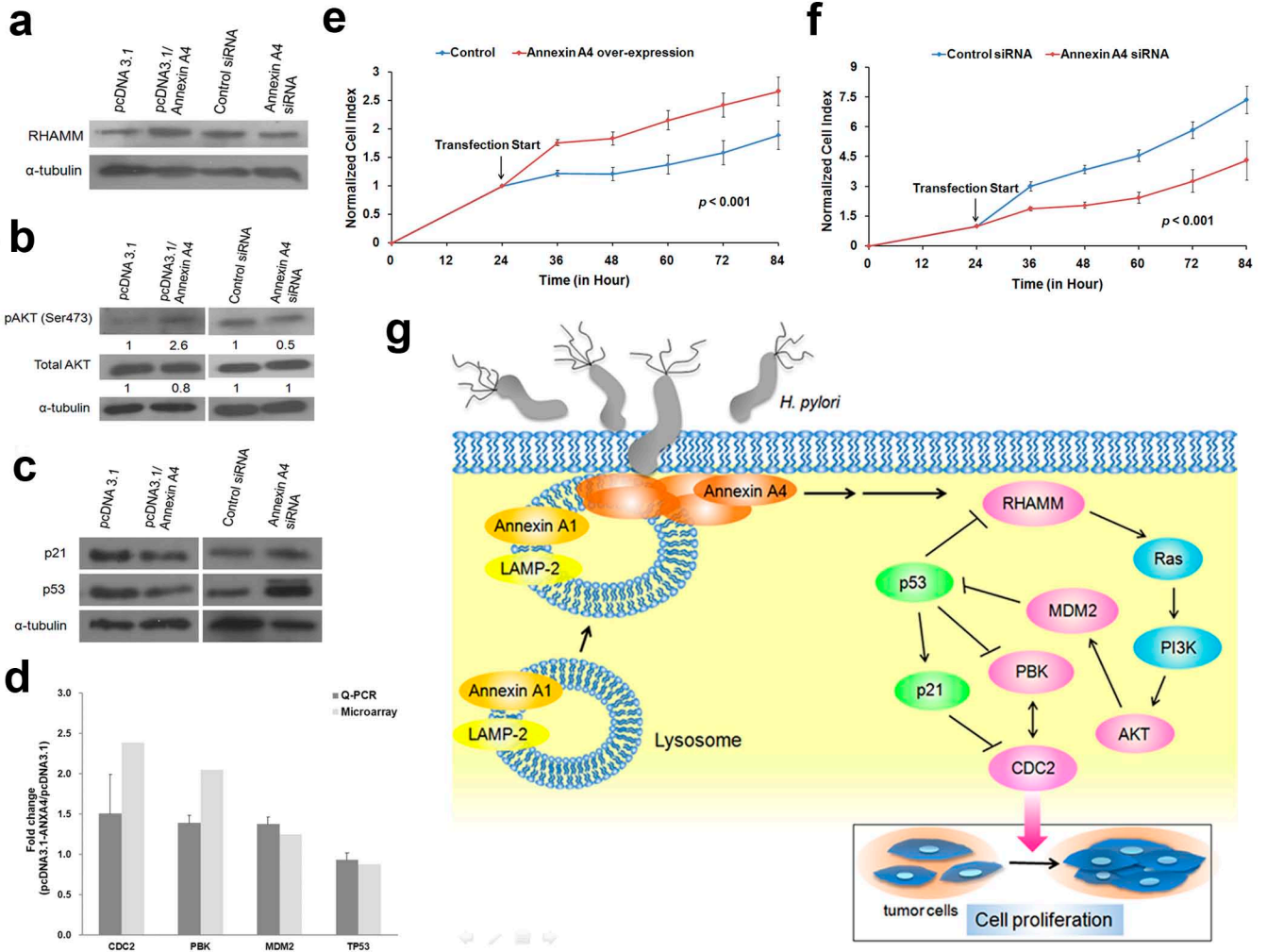
a
pcDNA 3.1
pcDNA3.1/ Annexin A4
Control siRNA
Annexin A4 siRNA
RHAMM
α-tubulin
b
pcDNA 3.1
pcDNA3.1/ Annexin A4
Control siRNA
Annexin A4 siRNA
pAKT (Ser473)
1 2.6 1 0.5
Total AKT
1 0.8 1 1
α-tubulin
c
pcDNA 3.1
pcDNA3.1/ Annexin A4
Control siRNA
Annexin A4 siRNA
p21
p53
α-tubulin
d
Q-PCR
Microarray
Fold change (pcDNA3.1-ANXA4/pcDNA3.1)
3.0
2.5
2.0
1.5
1.0
0.5
0.0
CDC2
PBK
MDM2
TP53
Gene
e
Control
Annexin A4 over-expression
Normalized Cell Index
Transfection Start
p < 0.001
Time (in Hour)
f
Control siRNA
Annexin A4 siRNA
Normalized Cell Index
Transfection Start
p < 0.001
Time (in Hour)
g
H. pylori
Annexin A4
Annexin A1
LAMP-2
Annexin A1
LAMP-2
Lysosome
RHAMM
Ras
p53
MDM2
PI3K
PBK
p21
AKT
CDC2
tumor cells
Cell proliferation